The Journal of Immunology

RESEARCH ARTICLE | MARCH 15 2008

Sporozoite-Mediated Hepatocyte Wounding Limits *Plasmodium* Parasite Development via MyD88-Mediated NF-κB Activation and Inducible NO Synthase Expression[1]

Ralph Torgler; ... et. al

J Immunol (2008) 180 (6): 3990–3999.
https://doi.org/10.4049/jimmunol.180.6.3990

Sporozoite-Mediated Hepatocyte Wounding Limits *Plasmodium* Parasite Development via MyD88-Mediated NF-κB Activation and Inducible NO Synthase Expression[1]

Ralph Torgler, Silayuv E. Bongfen, Jackeline C. Romero, Aubry Tardivel, Margot Thome, and Giampietro Corradin[2]

Plasmodium **sporozoites traverse several host cells before infecting hepatocytes. In the process, the plasma membranes of the cells are ruptured, resulting in the release of cytosolic factors into the microenvironment. This released endogenous material is highly stimulatory/immunogenic and can serve as a danger signal initiating distinct responses in various cells. Thus, our study aimed at characterizing the effect of cell material leakage during *Plasmodium* infection on cultured mouse primary hepatocytes and HepG2 cells. We observed that wounded cell-derived cytosolic factors activate NF-κB, a main regulator of host inflammatory responses, in cells bordering wounded cells, which are potential host cells for final parasite infection. This activation of NF-κB occurred shortly after infection and led to a reduction of infection load in a time-dependent manner in vitro and in vivo, an effect that could be reverted by addition of the specific NF-κB inhibitor BAY11-7082. Furthermore, no NF-κB activation was observed when *Spect*$^{-/-}$ parasites, which are devoid of hepatocyte traversing properties, were used. We provide further evidence that NF-κB activation causes the induction of inducible NO synthase expression in hepatocytes, and this is, in turn, responsible for a decrease in *Plasmodium*-infected hepatocytes. Furthermore, primary hepatocytes from *MyD88*$^{-/-}$ mice showed no NF-κB activation and inducible NO synthase expression upon infection, suggesting a role of the Toll/IL-1 receptor family members in sensing cytosolic factors. Indeed, lack of MyD88 significantly increased infection in vitro and in vivo. Thus, host cell wounding due to parasite migration induces inflammation which limits the extent of parasite infection.** ***The Journal of Immunology,*** **2008, 180: 3990–3999.**

A crucial step in the *Plasmodium* life cycle within the mammalian host is the infection of hepatocytes by sporozoites. Host cell infection is preceded by the traversal of several hepatocytes by the parasite. As a consequence, these hepatocytes are wounded due to membrane rupturing (1). It has been suggested that migration through host cells is necessary to establish infection and it is thought that during the process, sporozoites become fully activated for infection (2). In addition, wounded cells secrete hepatocyte growth factor, which renders neighboring cells more susceptible for infection and protects them also from apoptosis (3, 4). However, in contrast, it has been shown that sporozoites deficient in sporozoite microneme protein essential for cell traversal, which are disabled in cell-traversal motility, infect hepatocytes as well as wild-type parasites, which questions the absolute requirement of hepatocyte traversal for infection (5). Although many wounded cells survive this migration process, a considerable number become necrotic. In general, loss of membrane integrity results in an efflux of cytosolic factors into the surrounding medium, which is an acute danger signal capable of initiating inflammation (6, 7). As previously shown in fibroblasts and macrophages, unlike apoptotic cells in which the cell membranes stay intact for a prolonged period of time, necrotic cells which totally lose their membrane integrity, induce genes involved in inflammation and tissue repair (8). Different endogenous molecules, such as heat-shock proteins (hsp),[3] high mobility group box 1, and uric acid, have been identified to alert the immune system (9–11).

Toll-like receptors play a pivotal role in the initiation of an inflammatory response against various pathogens by recognizing conserved molecular patterns, called microorganism-associated molecular patterns (12). Toll-like receptors are expressed on different cell types and their importance has been investigated extensively on professional APCs, such as macrophages and dendritic cells. In addition to exogenous factors such as bacteria, viruses, and parasites, recent studies have also revealed a role of the Toll/IL-1 receptor family in regulating responses to endogenous factors (8, 13–15). Hepatocytes express multiple TLR family members and are therefore thought to be able to respond to various pathogens, but whether they are also responsive to endogenous factors is largely unknown (16). Toll/IL-1 receptor signaling involves the recruitment of common adaptor proteins, such as MyD88, IL-1 receptor-associated kinases, and TNF-α receptor-associated factor 6, which contribute to the activation of the IκB-kinase complex (12). The NF-κB heterodimer p50/p65 is held in an inactive state in the cytosol by its inhibitor IκBα (inhibitor of κBα). Toll/IL-1 receptor activated IκB-kinase phosphorylates IκBα leading to its

Department of Biochemistry, University of Lausanne, Epalinges, Switzerland

Received for publication March 7, 2007. Accepted for publication January 3, 2008.

The costs of publication of this article were defrayed in part by the payment of page charges. This article must therefore be hereby marked *advertisement* in accordance with 18 U.S.C. Section 1734 solely to indicate this fact.

[1] This work was supported by Lausanne University Institutional funds.

[2] Address correspondence and reprint requests to Dr. G. Corradin, Department of Biochemistry, Chemin des Boveresses 155, 1066 Epalinges, Switzerland. E-mail address: Giampietro.Corradin@unil.ch

[3] Abbreviations used in this paper: hsp, heat-shock protein; iNOS, inducible NO synthase; spz, sporozoites; sgm, homogenized salivary gland; PI, propidium iodide; DAPI, 4′,6-diamidino-2-phenylindole, dihydrochloride; *Pb*CSP, *P. berghei* circumsporozoite protein; EEFs, exoerythrocytic form; SN spz, supernatant of infected hepatocyte; SN MC, filtered supernatant of mechanically wounded cell; SMT, *S*-methylisothiourea sulfate; DN, dominant negative; CSP, circumsporozoite protein.

ubiquitination and proteasomal degradation. Active NF-κB is released, which translocates to the nucleus to initiate transcription of target genes, including proinflammatory cytokines and anti-apoptotic molecules (17).

An important proinflammatory molecule regulated by NF-κB is inducible NO synthase (iNOS) and its induction has been reported upon tissue destruction (18–20). iNOS-derived NO is a pleiotropic regulatory molecule involved in homeostasis, cytoprotection, cytotoxicity, tissue repair, and infection control. In particular, NO regulates the contraction of wounds, collagen biosynthesis, and cell proliferation, although the precise mechanism is unknown. In addition, several studies have demonstrated that NO is of central importance in anti-malarial liver immunity (21–23). Due to the many dramatic effects of iNOS activity, its expression has to be tightly controlled. iNOS expression is regulated at different levels such as gene induction, mRNA, and protein stability. However, an extensively described regulation takes place at the transcriptional level via activation of transcription factors that include NF-κB, AP-1, IRF-1, NF-IL-6, and STAT-1α (24).

In this study, we have investigated the role of sporozoite-induced hepatocyte wounding and its accompanied release of endogenous molecules on parasite development. We have found that leakage of cellular contents during the infection process with wild type but not *Spect*$^{-/-}$ parasites results in the rapid activation of NF-κB in hepatocytes bordering wounded cells. In addition, we demonstrate that NF-κB activation leads to the de novo synthesis of iNOS, which in turn eliminates a significant amount of intracellular parasites. We provide further evidence that iNOS expression is induced by members of the Toll/IL-1 receptor family, because *MyD88*$^{-/-}$ mouse primary hepatocytes showed no response. Our present data show that, *Plasmodium*-mediated hepatocyte wounding is unfavorable for the parasite due to the induction of an innate immune response, which partially limits infection.

Materials and Methods

Parasites

Anopheles stephensi mosquitoes were fed on *Plasmodium berghei* (ANKA strain)-harboring mice (parasitemia 2%) 3 to 5 days after eclosion. They were kept at 70% humidity at 21°C and were fed on a 10% glucose solution. One week after infection, they received a blood meal from uninfected mice. Twenty-one days after the infectious blood meal, sporozoites (spz) are isolated as follows: mosquitoes were first washed in 70% ethanol for 2 min, followed by two washes in DMEM containing 200 U/ml penicillin and 200 μg/ml streptomycin. Infected salivary glands of *Anopheles stephensi* mosquitoes were then isolated under a binocular microscope. To release the parasites, the isolated, infected salivary glands were homogenized in DMEM using a glass homogenizer. Additional centrifugation steps further purified the spz. As controls, homogenized salivary glands (sgm) of uninfected mosquitoes were used. To obtain inactivated sporozoites, freshly isolated spz were incubated at 56°C for 45 min as described before (4). *Spect*$^{-/-}$ parasites (5) were maintained as described above.

Cells

Mouse primary hepatocytes were isolated by a two-step collagenase perfusion of mouse liver lobules as previously described (25) with minor modifications. In brief, liver lobules were perfused for 10 min with Ca^{2+}-free HEPES buffer (pH 7.6) at 37°C followed by perfusion with type IV collagenase (Sigma-Aldrich) solution (Ca^{2+}-free HEPES buffer (pH 7.6) containing 0.04% type IV collagenase and 0.075% $CaCl_2 \blacksquare 2H_2O$) for another 5 min at 37°C. Resulting cells were purified over a 60% percoll gradient and washed twice by centrifugation at 800 rpm for 30 s. Because collagenase isolation of hepatocytes leads to NF-κB activation and iNOS mRNA expression, the cells were first cultured in standard medium (DMEM containing 10% FCS, 1% HEPES, 2 mM L-glutamine, 500 μM 2-ME, 100 U/ml penicillin, 100 μg/ml streptomycin) containing of 2 μM dexamethasone, a known suppressor of NF-κB and iNOS (26, 27). Cells were seeded on 1% gelatin coated plates. Five hours later, cells were washed and medium was replaced by standard medium only and cells were left for an additional 48 h before use. The human hepatocarcinoma cell line HepG2 was cultured in standard medium.

Generation of conditioned media

Conditioned medium was obtained by filtering (0.2 μm pore size) supernatants of cultured cells (2×10^5) incubated with *Plasmodium* sporozoites (10^5), or sgm or *Spect*$^{-/-}$ spz at 37°C for 1–3 h. No sporozoites were found in the conditioned medium as verified by microscopy. Alternatively, conditioned medium was generated from mechanically wounded cultured cells (10^6). Cells were wounded by scratching and left for 1–3 h at 37°C. Supernatant was filtered and used immediately.

Western blotting

A total of 10^6 HepG2 or mouse primary hepatocytes were either untreated or pretreated with 10 μM of the specific NF-κB inhibitor BAY11–7082 (Sigma-Aldrich) or DMSO as control for 1 h, followed by washing steps. After infection by 1×10^5 *Plasmodium berghei* sporozoites for different time periods, the cells were lysed in 200 μl NP40 lysis buffer (1% Triton X-100, 1% NP40, 20 mM Tris (pH 7.4), 150 mM NaCl, protease inhibitors, phosphatase inhibitors). Lysis was performed on ice for 10 min. Cell debris was removed by centrifugation (12,000 rpm, 4°C). Total protein concentration was assessed using the Bradford assay and 30 μg of protein sample was mixed with an equal volume of 3 × SDS-PAGE sample buffer. After electrophoresis on a 12% SDS-polyacrylamide gel and transfer to a nitrocellulose membrane, phosphorylated IκBα (Cell Signaling Technology) and α-tubulin (Sigma-Aldrich) were detected by using the corresponding primary Abs and secondary Abs. iNOS from mouse primary hepatocytes was detected using an anti-mouse iNOS Ab (BD Biosciences) and from HepG2 cells using an anti-human iNOS Ab (Santa Cruz Biotechnology). PMA- (Sigma-Aldrich) and ionomycin- (Calbiochem) treated Jurkat cells were used as a positive control for phospho-IκBα.

Luciferase reporter assay

Samples of 0.5×10^6 HepG2 cells (12-well plate) were transiently transfected using DOTAP Liposomal Transfection Reagent (Roche) with 5 μg of an NF-κB luciferase reporter construct (28) and 0.5 μg actin-β-Gal in DMEM supplemented with 10% FCS. After overnight incubation, the cells were washed, treated, and infected as described above for Western blot. Six hours later, the cells were lysed in 150 μl lysis buffer (0.2% Triton X-100, 92 mM KH_2PO_4, 0.91 mM K_2HPO_4, 1 mM DTT). Luciferase activity in the cell-free supernatant was assessed in a TD-20/20 Luminometer (Bio-Systems). Luciferase activity was normalized to β-galactosidase activity to correct for differences in transfection efficiency. In some experiments HepG2 cells were cotransfected with plasmids either overexpressing dominant negative, phosphorylation-deficient IκB (provided by Dr. Pascal Schneider, University of Lausanne, Switzerland), RelA (p65 subunit of NF-κB) (28) or dominant negative MyD88 (29), or with the empty vector pcDNA3.0 as control.

Determination of cellular wounding activity of sporozoites

Five $\times 10^4$ sporozoites were added to 2.5×10^5 HepG2 cells in presence of 10 μg/ml propidium iodide (PI). Fluorescent nuclei of PI positive cells, which represent the wounded cells, were recorded every 20 s with the microscope Axiovert 100 (Zeiss). To achieve the final movie, the data were processed using the program MetaMorphOffice version 7.0. Alternatively, HepG2 cells were incubated with either spz, inactivated sporozoites, sgm, or *Spect*$^{-/-}$ spz for 2 h. The cells were fixed and permeabilized with 100% methanol and all nuclei were stained with 4′,6-diamidino-2-phenylindole, dihydrochloride (DAPI) for 30 min. The percentage of wounded cells was calculated as follows: 100 × (PI positive nuclei/DAPI positive nuclei).

Determination of NF-κB translocation

Six $\times 10^4$ mouse primary hepatocytes were plated in 8-well Labtek chamber slides for 48 h. They were infected with 2×10^4 sporozoites for 2 h in the presence or absence of 10 μg/ml PI. Cells were washed in PBS and then fixed in 4% paraformaldehyde for 10 min. Cells were washed again and permeablized with 100% acetone for 1 min, followed by a blocking step (1% BSA in PBS for 30 min). Cells were then incubated with a polyclonal rabbit anti-p65 Ab (Santa Cruz Biotechnology) for 1 h at room temperature. Cells were washed twice and incubated with an anti-rabbit IgG Alexa Fluor 488-conjugated Ab in PBS-1% BSA for 1 h at room temperature. Cell nuclei were stained with DAPI for 30 min. Cells were examined with a fluorescence microscope (Axioplan; Zeiss).

Alternatively, cells were fixed in 1% glutaraldehyde first. Then they were incubated with a mouse Ab against the repeats of the *P. berghei* circumsporozoite protein (*Pb*CSP) followed by incubation with an anti-mouse IgG Cy3 Ab (Molecular Probes) in PBS-1% BSA for 1 h at room temperature to determine sporozoites outside cells. Next, cells were permeabilized with 100% methanol and p65 was stained as described above followed by the incubation with an anti-rabbit IgG Cy3 Ab (Molecular Probes) in PBS-1% BSA for 1 h at room temperature. Sporozoites were stained again with the anti-PbCSP Ab followed by an anti-mouse Alexa Fluor 488 Ab. Sporozoites which were single stained (Alexa Fluor 488) infected cells successfully.

Determination of number of infected cells

Six $\times$ 10^4 mouse primary hepatocytes were plated in 8-well Labtek chamber slides for 48 h. They were infected with 2 $\times$ 10^4 sporozoites for 2 h. Afterward, the cells were washed and either fixed with 1% glutaraldehyde or fixed and permeabilized with 100% methanol for 10 min. Sporozoites were then stained with an Ab against the repeats of the *Pb*CSP. The number of infected cells was calculated as follows: Number of sporozoites in methanol fixed wells − number of sporozoites in glutaraldehyde fixed wells.

Assessment of number of exoerythrocytic forms (EEFs)

HepG2 cells (10^5) or 6 $\times$ 10^4 mouse primary hepatocytes (wild type or *MyD88*$^{-/-}$) were plated in 8-well Labtek chamber slides for 24 or 48 h respectively, followed by infection with 2.5 $\times$ 10^4 sporozoites for 40 h, or as otherwise indicated. Staining of EEFs was performed as previously described (3). In brief, cells were first washed in PBS and then fixed in ice cold 100% methanol for 15 min on ice, followed by a blocking step (1% BSA in PBS for 30 min). After washing twice in PBS, cells were incubated with the monoclonal mouse anti-*Plasmodium* hsp70 Ab (2E6) (30) for 45 min at room temperature. Cells were again washed twice and incubated with an anti-mouse IgG Alexa Fluor 488-conjugated Ab in PBS-1% BSA for 45 min at room temperature. Cells were examined with a fluorescence microscope (DC200, Leica). EEFs in each well were counted and expressed as EEFs plus SD of duplicate wells.

^{51}Chromium release assay

A total of 10^5 HepG2 cells were plated per well in a 1% gelatin-coated 96-well plate and incubated overnight at 37°C. Cells were incubated with 75 μCi ^{51}Cr for 1 h. After washing repeatedly, the cells have been incubated with either spz, sgm, inactivated spz, or *Spect*$^{-/-}$ spz for 3 h. Alternatively, the cells were wounded mechanically. Supernatant was collected and released. ^{51}Cr was assessed with a gamma counter. The percentage of sporozoite-specific release of chromium was calculated as follows: [(experimental counts − spontaneous counts)/(maximum counts − spontaneous counts)] $\times$ 100.

Nitrite assay (Griess reaction assay)

NO is rapidly converted into the stable end products nitrite and nitrate. Total nitrite and nitrate concentrations of infected hepatocyte culture supernatants were measured by the Griess reaction. In brief, 100 μl of culture supernatant were mixed with 10 μl of 30% (w/v) $ZnSO_4$ solution to precipitate total proteins. After 30 min of incubation at room temperature, the solution was centrifuged at 3000 rpm for 5 min. To convert nitrate to nitrite, total supernatant was taken and incubated with 0.5 g of $CuSO_4$ coated cadmium beads for 60 min under shaking conditions. Supernatant was then centrifuged again and an equal volume of Griess reagent (0.5% sulfanilamide, 2.5% H_3PO_4, and 0.05% naphthylethylene diamine in H_2O) was added and incubated for 10 min at room temperature in the dark. Absorbance was assessed at 550 nm and compared with a standard curve obtained using sodium nitrite.

RT-PCR and real time PCR

A total of 10^6 primary hepatocytes were infected with 10^5 sporozoites for 24 h. Total RNA was isolated using TRIzol reagents according to the manufacturer's instructions (Sigma-Aldrich). Two μg of total RNA were reverse transcribed using a commercial kit as suggested by the manufacturer (Promega). The primers and PCR conditions have been described previously (31, 32). The primers used were β_2-microglobulin (β_2M) forward (5′-GGC TCGCTCGGTGACCCTAGTCTTT-3′) and reverse (5′-TCTGCAGGCGTAT GTATCAGTCTCA-3′), iNOS forward (5′-GCATGGACCAGTATAAGGC AAGCA-3′) and reverse (5′-GCTTCTGGTCGATGTCATGAGCAA-3′). The amplification conditions used were: 1 min at 94°C, 1 min at 60°C, and 1 min at 72°C for 30 cycles for β_2M; 1 min at 94°C, 1 min at 55°C, and 1 min at 72°C for 35 cycles for iNOS; and a final extension of 10 min at 72°C.

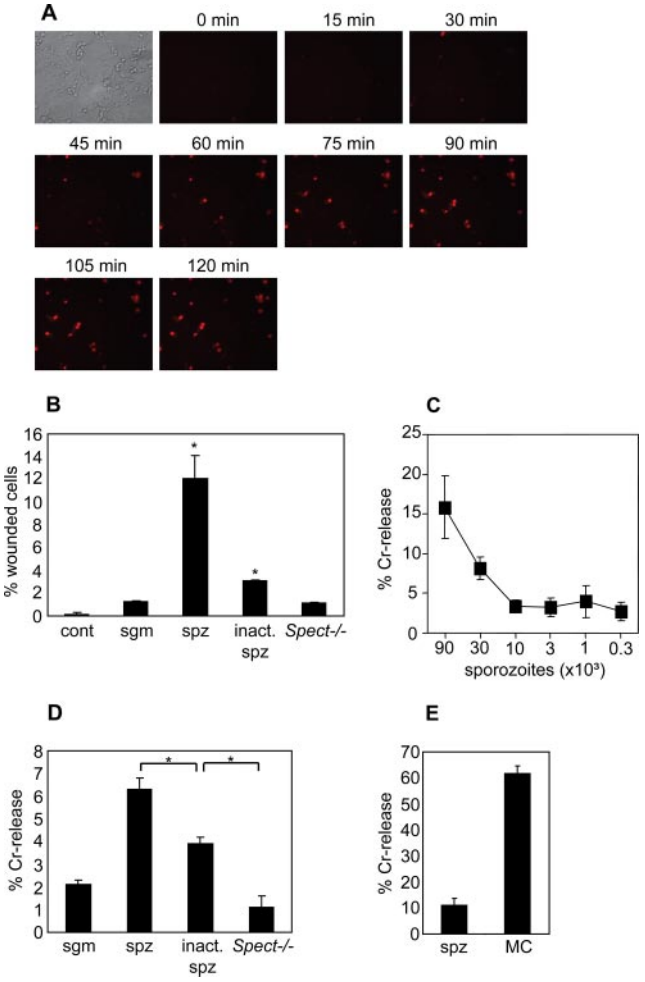

FIGURE 1. Release of cytosolic factors during hepatocyte infection process. *A*, Sporozoites were added to HepG2 cells in the presence of 10 μg/ml PI for 2 h. Every 20 s, the number of wounded cells (red) were recorded, whereas only selected time points are shown. *B*, HepG2 cells were treated or not with sporozoites (spz), salivary gland material (sgm), heat-inactivated spz (inact. spz), or *Spect*$^{-/-}$ spz for 2 h. The number of PI-positive nuclei and DAPI-positive nuclei (representing total cell number) were counted and the percentage of wounded cells was calculated. Mean values of duplicates ± SD of a representative experiment are shown. *, $p < 0.05$ (Student's *t* test). HepG2 cells were incubated with 75 μCi ^{51}Cr for 1 h, followed by several washes. Cells were then either infected with different numbers of sporozoites (*C*) or incubated with sgm, inactivated spz, or *Spect*$^{-/-}$ spz (*D*), or they were mechanically wounded and left for 3 h (*E*). Supernatant was harvested and radioactivity was assessed with a gamma counter. The percentage of ^{51}Cr-release was calculated and the mean values of triplicates ± SD of a representative experiment are shown. *, $p < 0.05$ (Student's *t* test).

In vivo assessment of parasite loads was performed with real time PCR as described previously with minor modifications (4). In brief, C57BL/6 mice were pretreated with BAY11-7082 (20 mg/kg body weight) or DMSO as control for 1 h i.p. followed by injection of 30′000 sporozoites i.v. Alternatively, C57BL/6 wild type or *MyD88*$^{-/-}$ mice (33) were injected with the same amount of sporozoites without pretreatment. Forty hours later, total livers were isolated and total RNA extracted. cDNA was synthesized as described above. The primers used were specific for the *P. berghei* 18S rRNA (forward: 5′-AAGCATTAAATAAAGCGAATACATC CTTAC-3′ and reverse: 5′-GGAGATTGGTTTTGACGTTTATGTG-3′). The DNA was amplified in the LightCycler 2.0 Instrument (Roche Diagnostics) using the program Roche LightCycler Run 5.32.

Assessment of parasitemia

Wild type, *MyD88*$^{-/-}$, or *iNOS*$^{-/-}$ (C57BL/6-Nos2tm1Lau; The Jackson Laboratory) mice were injected i.v. with 10^3 sporozoites. At different

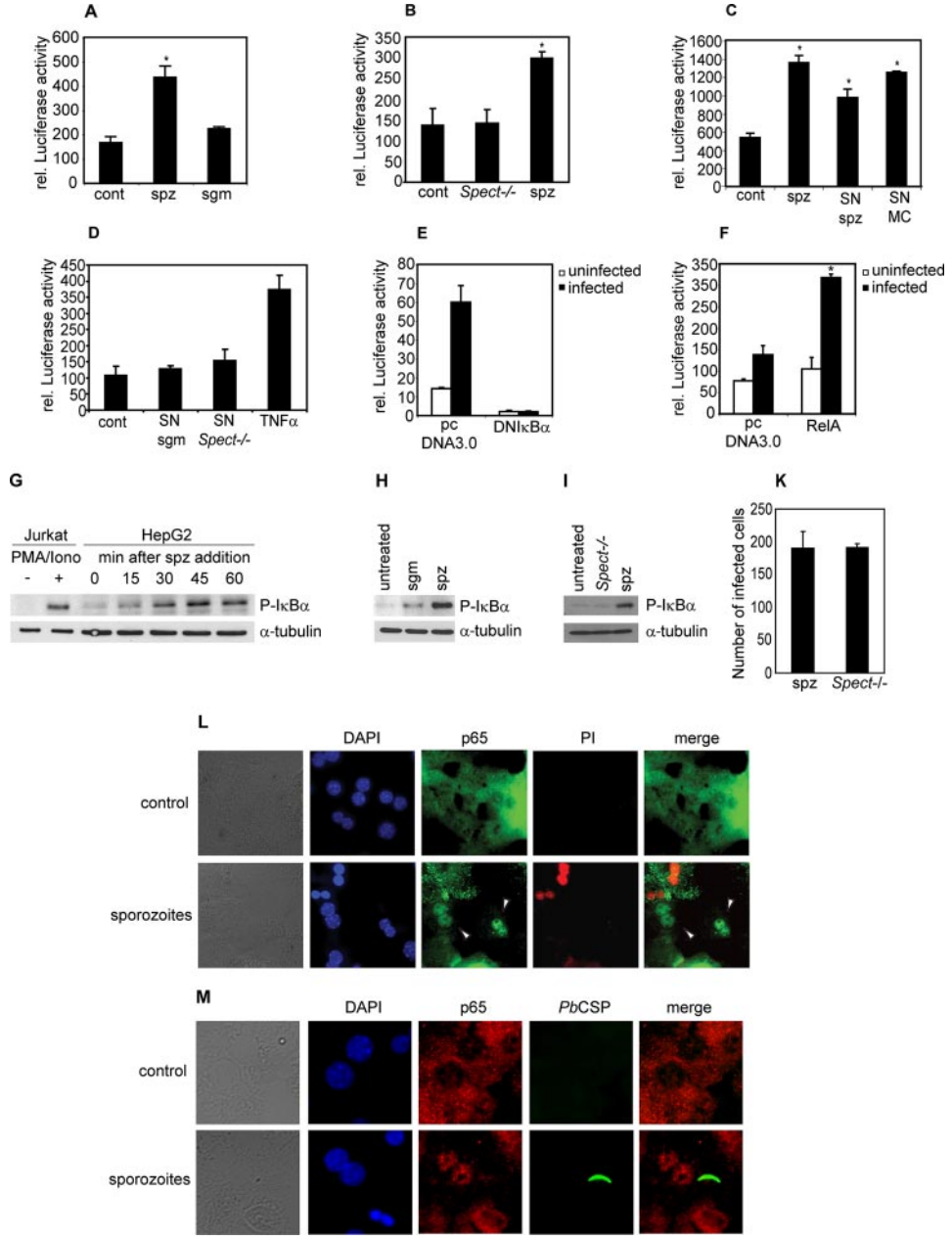

FIGURE 2. Sporozoite infection-mediated activation of NF-κB. HepG2 cells were transiently transfected with a NF-κB luciferase reporter construct and either left untreated (cont) or incubated with sporozoites (spz) or salivary gland material of uninfected mosquitoes (sgm) (*A*). *B*, Transfected HeG2 cells were left untreated or infected with wild-type spz or *Spect*$^{-/-}$ spz. *C*, Transfected HepG2 cells were left untreated or incubated with spz, filtered supernatant (SN) of infected hepatocytes or filtered supernatant of mechanically wounded cells (SN MC). *D*, Transfected HepG2 cells were left untreated or treated with TNF-α or incubated with conditioned media (SN) of sgm- or *Spect*$^{-/-}$ spz-treated hepatocytes. *E*, Cotransfection of a dominant negative IκBα expressing vector or vector control (pcDNA3.0) or cotransfection with a RelA (p65) expressing vector or vector control (pcDNA3.0) (*F*). After 6 h, luciferase activity was measured and normalized to β-galactosidase activity, to correct for differences in transfection efficiency. Mean values of triplicates + SD of a representative experiment are shown. *, $p < 0.05$ (Student's *t* test). *G*, HepG2 cells infected with sporozoites were harvested at the indicated time points and analyzed for phosphorylated IκBα (P-IκBα) by Western blot (30 μg/lane). Equal loading was confirmed by the detection of α-tubulin. Extracts from Jurkat cells either treated or untreated with PMA and ionomycin (50 ng/ml and 500 ng/ml, respectively) for 5 min were used as positive and negative controls (10 μg/lane). *H* and *I*, Mouse primary hepatocytes were either incubated or not with wild-type spz, sgm, or *Spect*$^{-/-}$ spz. Forty-five minutes later, P-IκBα was assessed by Western blot. Equal loading was confirmed by the detection of α-tubulin. *K*, Mouse primary hepatocytes were infected with either wild-type or *Spect*$^{-/-}$ spz for 2 h and the number of infected cells was assessed. Mean values of duplicates + SD of a representative experiment are shown. Mouse primary hepatocytes were either infected or not for 2 h followed by washing steps and fixation. *L*, Infection was conducted in presence of 10 μg/ml PI (red nuclei) to monitor wounded cells. All nuclei were stained with DAPI (blue). The NF-κB subunit p65 is shown in green; merge shows PI and p65. *M*, Nuclei are shown in blue, p65 in red, and sporozoite in green (*Pb*CSP). Merge shows p65 and *Pb*CSP.

time points, parasitemia was assessed by Giemsa-stained blood smear or alternatively by real-time PCR. Fifty microliters of total blood was taken and total RNA was isolated and reverse transcribed as mentioned above. The parasites were detected through 18S rRNA and normalization was done by β_2-microglobulin (β_2M) detection (as mentioned above).

Results

Sporozoite-mediated hepatocyte wounding releases cytosolic factors into the microenvironment

Sporozoites travel through several hepatocytes before infection and in the process cells are wounded by transient rupture of their membranes (1). Cells which fail to regain their membrane integrity die by necrosis, which results in an uncontrolled release of cytosolic factors into the extracellular environment. To monitor the kinetics of sporozoite-mediated cellular wounding, HepG2 cells were incubated with spz in the presence of PI, which is taken up by cells that lose their membrane integrity either transiently, or in the case of necrosis, permanently. PI positive nuclei (red) were recorded every 20 s. Fig. 1*A* shows distinct time points of the wounding kinetics. The first wounded cells appeared 30 min after addition of sporozoites and their numbers increased with time. Interestingly, the total wounding process, beginning from the appearance of the first wounded cell, lasted exactly 60 min. The percentage of wounded cells was assessed in HepG2 cells 2 h after addition of either spz, mosquito sgm as negative control, or heat-inactivated sporozoites or of sporozoites deficient in cell traversal motility (*Spect*$^{-/-}$). Fig. 1*B* shows, as expected, significant wounding occurred when incubated with spz, but not with sgm and *Spect*$^{-/-}$. Instead, incubation with heat-inactivated sporozoites led to a moderate but significant percentage of wounded cells. To assess the release of cytosolic factors following infection, HepG2 cells were labeled with radioactive ^{51}Cr, which was detected in the medium after cellular wounding. The amount of ^{51}Cr, and thus cytosolic factors, released was directly proportional to the number of sporozoites added to the cells (Fig. 1*C*). Compared with the incubation with spz, the treatment of HepG2 cells with sgm and *Spect*$^{-/-}$ did not lead to a significant release of cytosolic factors (Fig. 1*D*). Again, treatment with heat-inactivated sporozoites led to the release of a small, significant amount of endogenous material. Due to the residual traversal activity of heat-inactivated sporozoites, further control experiments were performed with *Spect*$^{-/-}$ sporozoites. As demonstrated in Fig. 1*E*, mechanical wounding of cells led to a 6-fold increase in ^{51}Cr-release compared with the release caused by sporozoites.

Cytosolic factors activate NF-κB in cells bordering wounded hepatocytes

Tissue damage and the accompanied release of endogenous factors provoke an inflammatory response mediated by NF-κB (8, 9). NF-κB is tightly regulated by the IκBα. From a variety of signals, IκBα is phosphorylated, ubiquitinated, and thus inactivated, resulting in the release and translocation of active NF-κB from the cytosol to the nucleus where transcription is initiated. To assess whether sporozoite infection activates NF-κB, HepG2 cells were transfected with a NF-κB luciferase reporter construct and either remained untreated, or were incubated with spz or sgm. Sporozoite infection caused a significant induction in NF-κB activity, unlike sgm treated cells (Fig. 2*A*). In addition, compared with wild-type spz, *Spect*$^{-/-}$ spz failed to activate NF-κB (Fig. 2*B*). To test whether sporozoite-induced hepatocyte damage, and thus the release of endogenous factors, activates NF-κB, conditioned media derived from filtered supernatant of infected hepatocytes (SN spz) or filtered supernatant of mechanically wounded cells (SN MC) were added to uninfected cells. Both conditions led to a significant activation of NF-κB (Fig. 2*C*). To exclude the introduction of unspecific activators during the generation process of the conditioned media used above, conditioned media from sgm- and *Spect*$^{-/-}$-treated cells were tested. None of these media activated NF-κB significantly (Fig. 2*D*). As positive control TNF-α-treated cells were used.

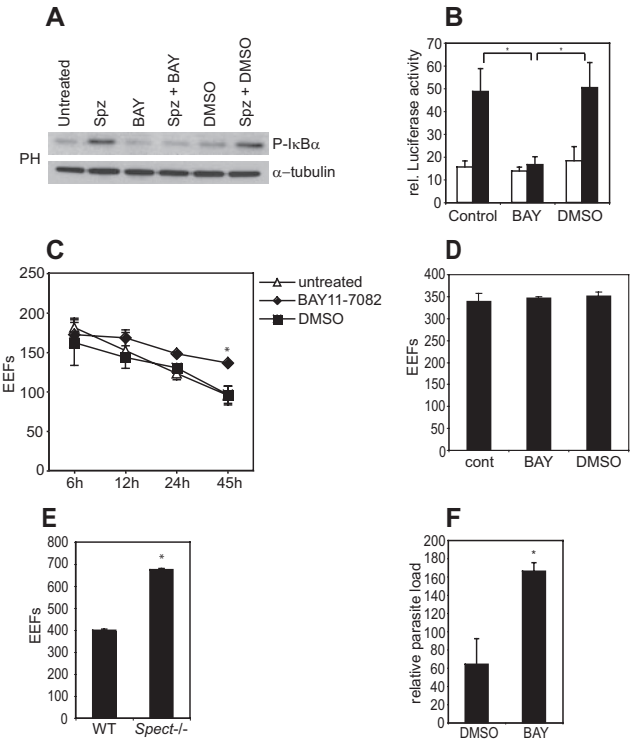

FIGURE 3. Inhibitory effect of Bay11-7082 on sporozoite-induced NF-κB activation and its beneficial effect on parasite development. *A*, Mouse primary hepatocytes (PH) were infected with sporozoites (Spz) either in presence or absence of the NF-κB inhibitor Bay11-7082 (BAY) or DMSO for 45 min. Aliquots were analyzed for p-IκBα by western blot (30 μg/lane). Equal loading was confirmed by the detection of α-tubulin. *B*, HepG2 cells were transiently transfected with a NF-κB reporter construct and infected either in the presence or absence of Bay11-7082 or DMSO. Luciferase activity was measured 6 h after infection. Parallel β-galactosidase activity was measured to correct for differencies in transfection efficiency. Mean values of triplicates + SD of a representative experiment are shown. *, $p < 0.05$. HepG2 cells were either left untreated or treated with 10 μM BAY11-7082 or DMSO (control) for 1 h followed by washing steps and infection with sporozoites. *C*, Number of wild-type exoerythrocytic forms in HepG2 cells (EEFs) was assessed at different time points after infection or EEFs of *Spect*$^{-/-}$ infected HepG2 cells was assessed 45 h post-infection using the anti-*Plasmodium* hsp70 Ab (2E6) (*D*). *, $p < 0.05$ (Student's *t* test). *E*, Mouse primary hepatocytes were infected either with wild-type or with *Spect*$^{-/-}$ sporozoites. Forty hours later, the number of EEFs was assessed. Mean values + SD of duplicates of a representative experiment are shown. *, $p < 0.05$ (Student's *t* test). *F*, 30′000 sporozoites were injected i.v. in C57/BL6 mice, which were either pretreated 1 h before with DMSO as control or with Bay11-7082 (20 mg/kg body weight) i.p. Liver infection was quantified 40 h post-infection by real-time RT-PCR. *, $p < 0.05$ (Student's *t* test).

Overexpression of dominant negative, phosphorylation-deficient IκBα blocked NF-κB completely (Fig. 2*E*). This demonstrates that NF-κB activation evolves via the classical pathway including phosphorylation and ubiquitination of IκBα followed by its degradation. In contrast, overexpression of RelA, the p65 subunit of the NF-κB heterodimer, led to a 2-fold increase in sporozoite-induced NF-κB activation over that observed in control (pcDNA3.0) transfected cells (Fig. 2*F*).

The kinetics of sporozoite-induced phosphorylation of IκBα in hepatocytes showed that IκBα phosphorylation could be

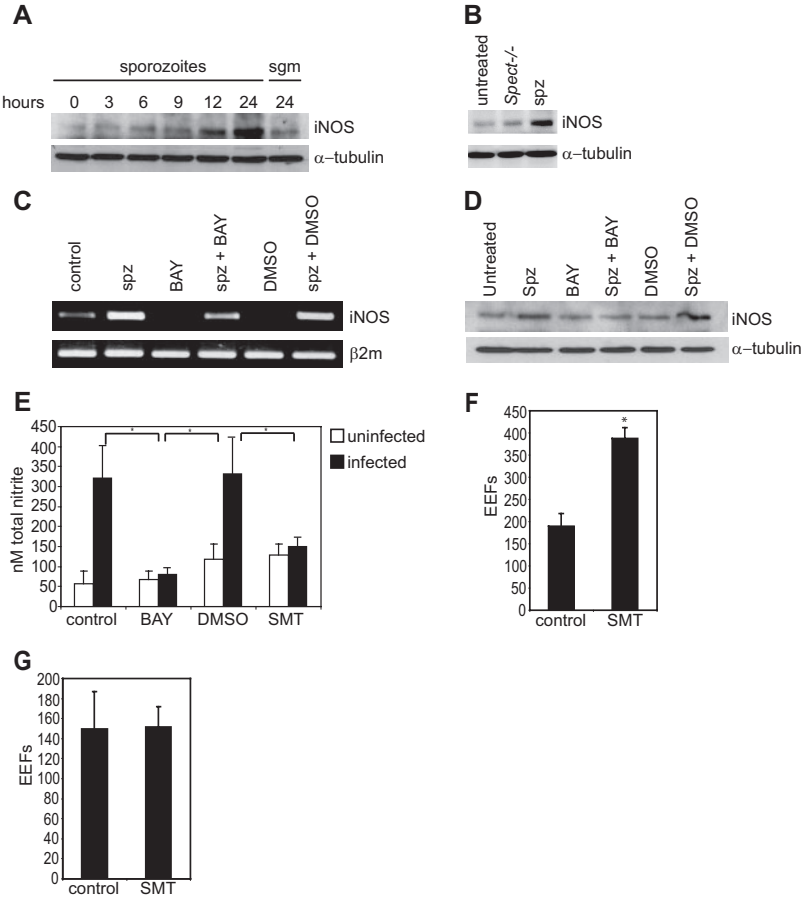

FIGURE 4. NF-κB-dependent expression of iNOS modulates the number of infected cells. *A*, HepG2 cells were incubated with sporozoites or salivary gland material of uninfected hepatocytes (sgm) for the indicated time points. iNOS expression was assessed by Western blot. Equal loading was confirmed by the detection of α-tubulin. *B*, Mouse primary hepatocytes were either left untreated or incubated with wild-type or *Spect*$^{-/-}$ sporozoites. iNOS expression was assessed 24 h later by Western blot. Mouse primary hepatocytes were left untreated or treated with 10 μM BAY11-7082, DMSO, or 12 h post-infection with 20 μM S-methylisothiourea sulfate (SMT), respectively. Twenty-four hours after sporozoite infection, iNOS expression was assessed by RT-PCR (*C*) and Western blot (*D*) and iNOS enzyme activity was scored by the nitrite assay (*E*). Mouse primary hepatocytes were either left untreated or treated with 20 μM SMT 12 h after infection with sporozoites. Forty hours post infection the number of wild-type exoerythrocytic forms (EEFs) (*F*) or *Spect*$^{-/-}$ EEFs (*G*) were assessed. Mean values of duplicates of a representative experiment + SD are shown. *, $p < 0.05$ (Student's *t* test).

detected as early as 30 min after infection of HepG2 cells with sporozoites (Fig. 2*G*). As a positive control for IκBα phosphorylation, we used Jurkat cells treated with PMA/ionomycin for 5 min (Fig. 2*E*, first two lanes). In agreement with our observation in HepG2 cells, sporozoites but not sgm or *Spect*$^{-/-}$ sporozoites led to phosphorylation of IκBα in mouse primary hepatocytes (Fig. 2, *H* and *I*).

To demonstrate that wild-type and *Spect*$^{-/-}$ sporozoites equally infect hepatocytes, and that NF-κB activation does not depend on infectivity, the number of infected cells was assessed 2 h post-infection. No differences in the number of infected hepatocytes was scored between wild type and *Spect*$^{-/-}$ sporozoites (Fig. 2*K*).

To assess the ability of hepatocytes bordering injured cells to activate NF-κB in response to infection, we analyzed the subcellular localization of the p65 subunit of the NF-κB heterodimer in infected mouse primary hepatocytes. In uninfected cells, p65 (green) is predominantly located in the cytoplasm (Fig. 2*L*). However, 2 h after addition of sporozoites, nuclear translocation of p65 (white arrows) was observed in cells neighboring wounded cells (PI stained nuclei; red) but not in distant cells. Interestingly, >90% of wounded cells did not show any nuclear p65. In addition, their nuclei were often smaller than the nuclei of healthy cells. We observed that cells containing translocated p65 (red) were potential target cells for final parasite (green) infection (Fig. 2*M*). In fact, we found that NF-κB was activated in around 35% of infected hepatocytes.

These observations showed that activation of NF-κB is an immediate early response induced by hepatocyte-derived factors which are released during the process of sporozoite cell traversal.

Sporozoite infection-mediated NF-κB activation negatively interferes with parasite development

Recently, the chemical compound Bay11-7082 has been described as being a selective inhibitor of cytokine-induced IκBα phosphorylation (34). We therefore analyzed its effect on *Plasmodium*-induced IκBα phosphorylation. Bay11-7082 potently inhibited parasite-mediated IκBα phosphorylation in mouse primary hepatocytes, while treatment with solvent alone (DMSO) showed no reduction of phosphorylated IκBα (Fig. 3*A*). As expected, Bay11-7082 but not DMSO inhibited parasite-induced NF-κB luciferase activity in HepG2 cells (Fig. 3*B*). To investigate the influence of *Plasmodium*-mediated NF-κB activation on liver-stage development of the parasite, we infected HepG2 cells, which were either untreated or treated with BAY11-7082 or DMSO and assessed the number of *Plasmodium*-infected cells at different time points after infection. Results demonstrated that in untreated or control-treated (DMSO) hepatocytes, the number of EEFs decreased with time (Fig. 3*C*). To the contrary, in BAY11-7082-treated hepatocytes the loss of infected hepatocytes was less pronounced. In contrast, the number of *Spect*$^{-/-}$ EEFs did not change between untreated, BAY11-7082 or DMSO treated cells 45 h post-infection (Fig. 3*D*). Because *Spect*$^{-/-}$ sporozoites fail to activate NF-κB, we compared the number of EEFs between wild-type and *Spect*$^{-/-}$ sporozoites 40 h post-infection. Interestingly, the number of *Spect*$^{-/-}$ EEFs was significantly higher compared with the number of wild-type EEFs (Fig. 3*E*).

To assess the significance of NF-κB in vivo, we infected mice with 30′000 sporozoites, which were either pretreated with DMSO as a control or with the IκBα phosphorylation inhibitor Bay11-7082 for 1 h. Liver infection was assessed 40 h post-infection by

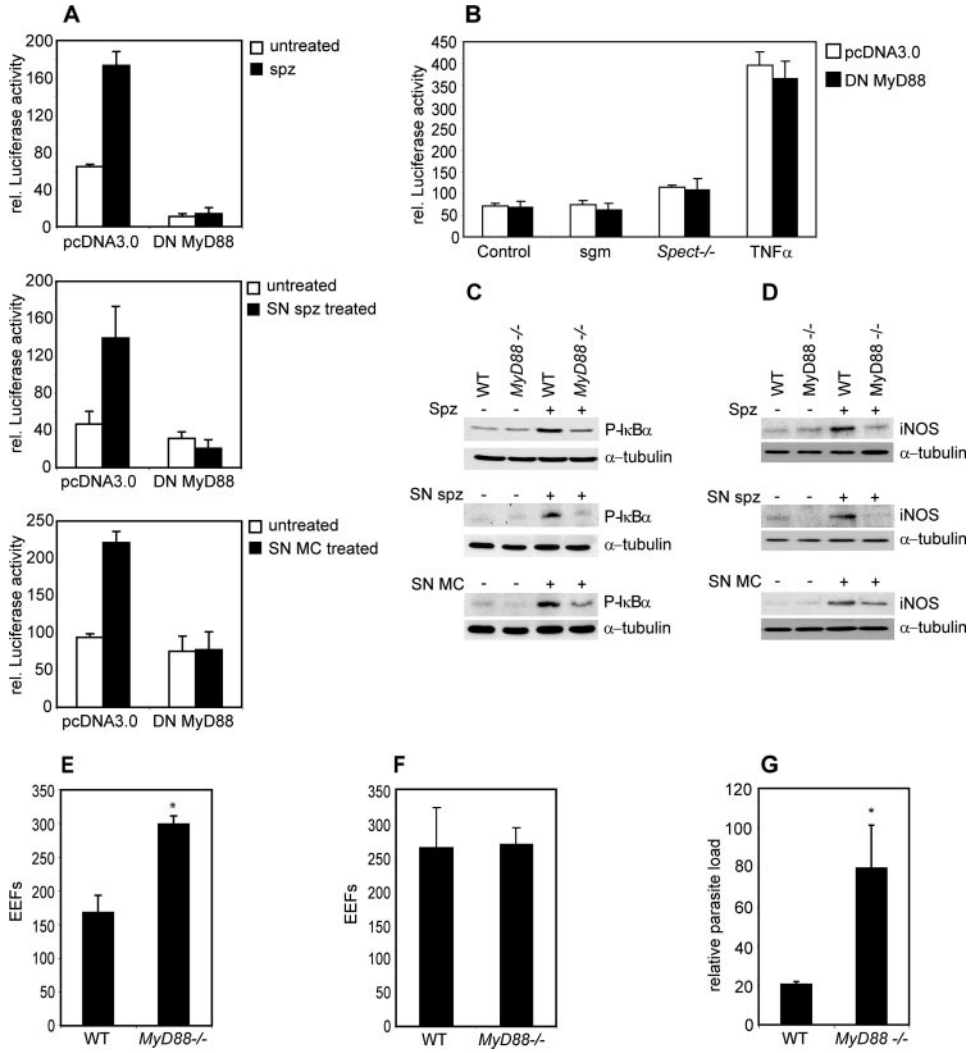

FIGURE 5. Hepatocyte wounding-mediated activation of NF-κB and iNOS expression require MyD88. HepG2 cells were transiently transfected with a NF-κB luciferase reporter construct and either a dominant negative MyD88 (DN MyD88) expressing vector or a vector control (pcDNA3.0). *A*, Afterward, they were infected with sporozoites (spz), or treated with filtered supernatant (SN) of infected hepatocytes (SN spz) or SN of mechanically wounded cells (SN MC) or treated with sgm or *Spect*$^{-/-}$ sporozoites. *B*, As positive control, TNF-α-treated cells were used. Six hours later, luciferase activity was measured and normalized to β-galactosidase activity, to correct for differences in transfection efficiency. Mean values of triplicates + SD of a representative experiment are shown. Wild-type (WT) and *MyD88*$^{-/-}$ mouse primary hepatocytes were either left untreated or infected with spz, treated with SN spz or SN MC. P-IκBα (*C*) and iNOS (*D*) were assessed by Western blot. Equal loading was confirmed by the detection of α-tubulin. The number of wild-type exoerythrocytic forms (EEFs) (*E*) and *Spect*$^{-/-}$ EEFs (*F*) were assessed 40 h post infection in wild-type and *MyD88*$^{-/-}$ mouse primary hepatocytes. Mean values of duplicates + SD of a representative experiment are shown. ∗, $p < 0.05$ (Student's *t* test). *G*, 30′000 sporozoites were injected i.v. in wild-type and *MyD88*$^{-/-}$ mice. Liver infection was quantified 40 h post-infection by real-time RT-PCR. ∗, $p < 0.05$.

real-time PCR. Bay11-7082 significantly enhanced liver infection compared with control (DMSO)-treated mice (Fig. 3*F*).

Taken together, these results demonstrated that there is a hepatocyte-mediated response against *Plasmodium* infection which is regulated by NF-κB, and that NF-κB activation can contribute to the reduction of parasite infection.

NF-κB-regulated iNOS expression in hepatocytes reduces the number of infected cells

Increased iNOS expression has been observed upon tissue wounding (18–20). Indeed, iNOS-derived NO regulates wound contraction, collagen formation, and cell proliferation. In addition, NO has strong antimicrobial activity and its importance in antimalarial immunity has been well documented (22, 23). To assess the ability of sporozoites to induce iNOS expression in hepatocytes, HepG2 cells were incubated with either sporozoites or salivary gland material of uninfected mosquitoes (sgm) and iNOS expression was assessed at different time points. Significant sporozoite-mediated iNOS expression was detectable in HepG2 cells as early as 12 h post-infection, and became much more pronounced at 24 h after infection, while iNOS induction in cells treated with sgm only was close to background levels (Fig. 4*A*). In addition, incubation with *Spect*$^{-/-}$ sporozoites failed to activate iNOS expression (Fig. 4*B*). Although it had been previously shown that *P. falciparum* induces iNOS expression in human primary hepatocytes (35), the molecular regulation of *Plasmodium*-mediated iNOS expression was not explored. To determine the extent to which this iNOS expression and activity is dependent on NF-κB, we infected primary mouse hepatocytes, either in presence or absence of BAY11-7082 or DMSO, and analyzed iNOS induction by RT-PCR (Fig. 4*C*), Western blot (Fig. 4*D*), and iNOS enzyme activity by the nitrite assay (Fig. 4*E*). All three methods revealed that iNOS expression

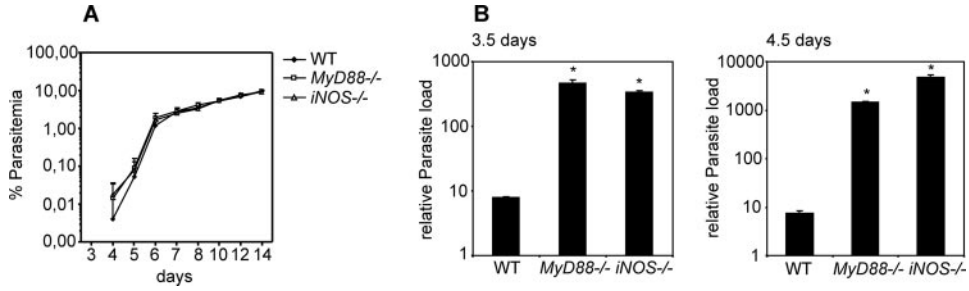

FIGURE 6. Higher parasitemia level in MyD88$^{-/-}$ and iNOS$^{-/-}$ mice compared with wild-type mice during early blood-stage infection. *A*, A total of 10^3 sporozoites were injected i.v. into either wild-type, *MyD88*$^{-/-}$ or *iNOS*$^{-/-}$ mice (five mice/group). Parasitemia of each mouse was assessed by a Giemsa-stained blood smear after inoculation on the days indicated. The values shown represent the mean parasitemia +/− SD. *B*, Early parasitemia was assessed by real-time PCR, 3.5 and 4.5 days post inoculation. Relative parasite load is represented by parasite 18S rRNA. An asterisk indicates $p < 0.05$.

in hepatocytes after sporozoite infection was NF-κB dependent. Furthermore, Fig. 4*E* showed that sporozoite-induced iNOS enzyme activity can be blocked selectively by the chemical inhibitor *S*-methylisothiourea sulfate (SMT). To assess whether sporozoite-induced NO production kills intrahepatic parasites, we infected mouse primary hepatocytes with sporozoites and treated the cells with SMT, 12 h post-infection. The total number of infected hepatocytes was assessed by immunostaining 40 h later. As illustrated in Fig. 4*F*, the number of wild-type EEFs was significantly higher in cells treated with SMT compared with untreated cells, most likely because SMT prevented the antimicrobial activity of iNOS. In contrast, no difference in the number of *Spect*$^{-/-}$ EEFs was observed between untreated cells and cells treated with SMT (Fig. 4*G*).

MyD88-dependent activation of NF-κB and iNOS expression upon hepatocyte wounding

TLRs play a crucial role in the initiation of an effective immune response against various pathogens (12). In addition, TLRs sense endogenous self Ags such as necrotic cell-derived factors, which provoke inflammation (8). Signaling of distinct TLRs is dependent on the adapter protein MyD88 (12). Therefore, to test whether sporozoite-mediated NF-κB activation is TLR-dependent, we overexpressed dominant negative (DN) MyD88 in HepG2 cells and infected them (spz), or treated them with conditioned media of either infected hepatocytes (SN spz) or mechanically wounded cells (SN MC). Unlike in control transfected cells (pcDNA3.0), overexpression of DN MyD88 inhibited spz-, SN spz-, and SN MC-induced NF-κB activation completely (Fig. 5*A*). NF-κB activation after sgm and *Spect*$^{-/-}$ treatment was compared between control cells and DN MyD88 overexpressing cells. As expected sgm and *Spect*$^{-/-}$ treatment did not lead to activation of NF-κB (Fig. 5*B*). As positive control, TNF-α-treated cells were used. To further confirm the results observed in HepG2 cells, we infected wild-type or *MyD88*$^{-/-}$ mouse primary hepatocytes and detected endogenous levels of P-IκBα (Fig. 5*C*) and iNOS protein expression (Fig. 5*D*). Compared with wild-type hepatocytes, in *MyD88*$^{-/-}$ cells the levels of P-IκBα and iNOS were similar to background levels after spz infection or SN spz or SN MC treatment. The number of infected cells was assessed in wild-type and *MyD88*$^{-/-}$ hepatocytes 40 h post-infection. Consistent with our expectations, the number of wild-type EEFs in *MyD88*$^{-/-}$ cells was significantly higher compared with wild-type cells (Fig. 5*E*), whereas the number of *Spect*$^{-/-}$ EEFs did not differ between wild type cells and *MyD88*$^{-/-}$ cells (Fig. 5F). To assess the significance of MyD88 in vivo, wild-type and *MyD88*$^{-/-}$ mice were infected with 30′000 sporozoites and the liver infection rate was assessed 40 h post-infection by real-time PCR. As predicted, the level of infection was significantly higher in *MyD88*$^{-/-}$ mice than in wild-type mice (Fig. 5*G*). Our data clearly demonstrate that sporozoite-mediated cellular wounding and its associated release of cytosolic factors result in activation of NF-κB and iNOS expression through the activation of TLRs, thereby limiting the number of infected cells.

MyD88 and iNOS influences early blood-stage infection

To assess whether the MyD88- and iNOS-dependent decrease in liver infection influences the course of the disease, we infected either wild-type, iNOS-, or MyD88-deficient mice with 1000 sporozoites and assessed parasitemia. As shown in Fig. 6*A*, parasitemia is similar in all three mouse strains tested except at early time points where parasitemia is significantly higher in MyD88 and iNOS mice compared with wild-type mice as confirmed by real-time PCR (Fig. 6*B*).

Discussion

The role of hepatocyte traversal by sporozoites in malaria infection has been addressed in the past. A current model claims that cell traversal is beneficial and necessary for final infection, because it triggers the switch from cell passage to cell invasion motility (2). In support of this model, studies have shown that hepatocyte growth factor, secreted by wounded cells, binds its receptor Met on neighboring cells and subsequently renders them susceptible for infection (3). However, the dependence of infection on host factors released during cell traversal has been disproved by *Spect*$^{-/-}$ sporozoites that are deficient in cell traversal, but infect hepatocytes just as well as wild-type sporozoites (5). In support of the latter findings, we show in this study that cell traversal by sporozoites has a detrimental effect on parasite survival, because non-traversed hepatocytes have the ability to respond to released host factors resulting in a NF-κB-dependent innate immune response and reduced infection. Indeed, NF-κB activation was found to be an early event that occurred at the same time as appearance of the first wounded cells (Figs. 1*A* and 2*G*), suggesting that rather than the parasite itself, the cell traversal activity of the sporozoites is the essential stimulus for the immune response. This is supported by the observation that compared with wild-type sporozoites, *Spect*$^{-/-}$ sporozoites failed to activate NF-κB significantly (Fig. 2, *B* and *I*). Surprisingly, heat-inactivated sporozoites still retain residual traversing activity and could not serve as a proper control in these studies (Fig. 1, *B* and *D*). Our observations therefore exclude the possibility that sporozoite-secreted proteins alone, such as the CSP and thrombospondin-related adhesion protein, or a simple contact of parasite and host cells may be a sufficient trigger to activate NF-κB. The liver has long been considered a tolerogenic organ that favors the induction of peripheral tolerance because it is in constant contact with microbial products derived from the gut.

This may explain the unresponsiveness of hepatocytes to *Spect*$^{-/-}$ sporozoites. In contrast, tissue damage can break this tolerance, generating an environment that promotes tissue recovery and a response against pathogens. Indeed, supernatant derived from mechanically wounded cells activated NF-κB to a similar level as supernatant from sporozoite-damaged hepatocytes, which showed a 6-fold lower ^{51}Cr release (Figs. 1*E* and 2*C*). We can therefore hypothesize that cell wounding initiates NF-κB activation and breaks tolerance, thus sensitizing hepatocytes to the presence of parasites, leading to more NF-κB activation in a synergistic manner. The difference in ^{51}Cr release between mechanically wounded cells and sporozoite-damaged hepatocytes may not be indicative for the actual amount of NF-κB activating material. Alternatively, mechanical wounding of cells differs from parasite-mediated wounding which may result in the release of different hepatocyte factors with distinct efficiencies in activating NF-κB. A proteomic approach to address this question is envisaged.

It is interesting to note that NF-κB was not activated in wounded cells (Fig. 2*L*), thus excluding an autocrine activation, and this might be an indication of lethal damage. Although it has been shown that many cells are able to reseal their membranes upon injury, their subcellular architecture is disrupted (36). Therefore, it is very doubtful whether sporozoite-traversed cells fully recover. In addition, wounded cells contain free sporozoite-derived proteins in the cytoplasm, which might potently interfere with important host cell functions. Indeed, recently it has been shown that overexpression of CSP antagonizes NF-κB translocation to the nucleus in infected cells upon TNF-α stimulation, which consequently inhibits the expression of proinflammatory molecules (37). This seems to contradict our observations. However, whereas the CSP in wounded cells is freely in the cytosol and thus able to act immediately, the situation in an infected neighboring cell is different in the sense that the CSP has to be actively transported through the parasitophorous vacuole to block the translocation of activated NF-κB in the cytosol. Our data suggest that the signal induced by endogenous factors evolves chronologically earlier than that associated with CSP. CSP however may control the magnitude of the NF-κB response and block later NF-κB-inducing stimuli.

NF-κB activation evolved in a MyD88-dependent manner indicating the so-far unknown competency of hepatocytes to respond to endogenous factors via TLR family members (Fig. 5, *A* and *C*). However, further work is needed to elucidate which members of the TLR family are implicated in NF-κB activation during sporozoites infection. In addition, we cannot exclude a role of IL-1R and IL-18R in NF-κB activation, because downstream signaling pathways of these receptors also require MyD88.

The activation of NF-κB and subsequent expression of iNOS upon hepatocyte wounding eliminated about a third of all exoerythrocytic forms. This decrease is in accordance with the observation that NF-κB was activated in ~35% of infected hepatocytes (Fig. 2*M*). These cells were predominantly directly bordering wounded cells (Fig. 2*L*). Consistently, because *Spect*$^{-/-}$ sporozoites do not activate NF-κB, their number of EEFs was significantly higher than that of the wild-type-derived EEFs. This result conflicts the observations by Ishino et al. (5) where the number between wild-type and *Spect*$^{-/-}$ EEFs did not differ. This discrepancy can be explained by the fact that different reagents were used to assess the number of exoerythrocytic forms. Whereas Ishino et al. (5) used the CSP as an indicator for EEFs, parasite-expressed Hsp was used in this study. Hsp is expressed in sporozoites in low quantities and we observed that during EEF development the expression is greatly enhanced (data not shown). Therefore, using the Hsp allows a more accurate assessment of EEF development than using the CSP, which is expressed exclusively on sporozoites. The NF-κB- and iNOS-mediated decrease in liver infection is reflected in the significantly higher parasitemia in iNOS- and MyD88-deficient mice compared with wild-type mice at early time points (Fig. 6*B*).

The partial inhibition of parasite development discussed above is in line with the notion of concomitant evolution of pathogens and hosts. In fact, various mechanisms have evolved to strike a balance between survival and death of pathogens and hosts. One of these mechanisms is the interference with TLR signaling to control the magnitude of the immune response and so avoid detrimental outcomes, such as severe host tissue destruction or total eradication of the pathogen. Therefore, TLR-mediated signaling events contain negative feedback mechanisms. For example, soluble decoy TLRs (sTLR-2/-4) antagonize ligand binding and potently attenuate TLR-induced effector functions (38, 39). Different intracellular negative regulators have been uncovered such as MyD88s, IRAKM, TOLLIP, A20, SOCS1, PI3K, and NOD2 (40–42). Thus, pathogens may target these molecules to ensure their survival. Interestingly, PI3K is activated in hepatocytes early upon infection (4). To date, it is unclear whether it might be a candidate to limit a TLR-mediated immune response against the parasite. As already discussed above, an additional candidate is the CSP (37).

The *Spect*$^{-/-}$ protein is essential for the sporozoite to cross the sinusoidal cell layer to reach the hepatocytes. However, the reason why sporozoites continue traversing hepatocytes remains unclear. Even though *Spect*$^{-/-}$ sporozoites infect hepatocytes just as well as wild-type sporozoites (Fig. 2*K*), we cannot exclude the possibility that sporozoites become activated for final infection through host cell traversal activity as suggested by a previous study (2). It is possible that regulated exocytosis of proteins induced by hepatocyte traversal may be necessary to antagonize the effect of Spect. An alternative hypothesis is that traversal activity is used by sporozoites to divert the immune system from the final infected hepatocytes. Indeed, traversed hepatocytes have been shown to present the CSP to specific T cells and undergo apoptosis (43). The price to pay for this possible decoy mechanism is a lower parasite infection rate.

In summary, pathogen-mediated tissue destruction induces an innate immune response and *Plasmodium* sporozoite-mediated hepatocyte wounding is no exception, with the consequence of activating nearby hepatocytes that respond by limiting the extent of parasite infection.

Acknowledgments

We thank Dr. Thomas Brunner and Dr. Pascal Schneider for providing expression and reporter plasmids, Dr. Olivier Gaide and Dr. Moriya Tsuji for Abs, Dr. Jürg Tschopp for providing the *MyD88*$^{-/-}$ mice and Shizuo Akira for the generation of these mice, Dr. Robert Ménard for the *Spect*$^{-/-}$ parasites and Masao Yuda for generation of these parasites, and Dr. Stephan Duss for technical assistance.

Disclosures

The authors have no financial conflict of interest.

References

1. Mota, M. M., G. Pradel, J. P. Vanderberg, J. C. Hafalla, U. Frevert, R. S. Nussenzweig, V. Nussenzweig, and A. Rodriguez. 2001. Migration of *Plasmodium* sporozoites through cells before infection. *Science* 291: 141–144.
2. Mota, M. M., J. C. Hafalla, and A. Rodriguez. 2002. Migration through host cells activates *Plasmodium* sporozoites for infection. *Nat. Med.* 8: 1318–1322.
3. Carrolo, M., S. Giordano, L. Cabrita-Santos, S. Corso, A. M. Vigario, S. Silva, P. Leiriao, D. Carapau, R. Armas-Portela, P. M. Comoglio, et al. 2003. Hepatocyte growth factor and its receptor are required for malaria infection. *Nat. Med.* 9: 1363–1369.
4. Leiriao, P., S. S. Albuquerque, S. Corso, G. J. van Gemert, R. W. Sauerwein, A. Rodriguez, S. Giordano, and M. M. Mota. 2005. HGF/MET signalling protects *Plasmodium*-infected host cells from apoptosis. *Cell. Microbiol.* 7: 603–609.

5. Ishino, T., K. Yano, Y. Chinzei, and M. Yuda. 2004. Cell-passage activity is required for the malarial parasite to cross the liver sinusoidal cell layer. *PLoS Biol.* 2: E4.
6. Skoberne, M., A. S. Beignon, and N. Bhardwaj. 2004. Danger signals: a time and space continuum. *Trends Mol. Med.* 10: 251–257.
7. Matzinger, P. 1994. Tolerance, danger, and the extended family. *Annu. Rev. Immunol.* 12: 991–1045.
8. Li, M., D. F. Carpio, Y. Zheng, P. Bruzzo, V. Singh, F. Ouaaz, R. M. Medzhitov, and A. A. Beg. 2001. An essential role of the NF-κB/Toll-like receptor pathway in induction of inflammatory and tissue-repair gene expression by necrotic cells. *J. Immunol.* 166: 7128–7135.
9. Basu, S., R. J. Binder, R. Suto, K. M. Anderson, and P. K. Srivastava. 2000. Necrotic but not apoptotic cell death releases heat shock proteins, which deliver a partial maturation signal to dendritic cells and activate the NF-κB pathway. *Int. Immunol.* 12: 1539–1546.
10. Shi, Y., J. E. Evans, and K. L. Rock. 2003. Molecular identification of a danger signal that alerts the immune system to dying cells. *Nature* 425: 516–521.
11. Scaffidi, P., T. Misteli, and M. E. Bianchi. 2002. Release of chromatin protein HMGB1 by necrotic cells triggers inflammation. *Nature* 418: 191–195.
12. Kaisho, T., and S. Akira. Toll-like receptor function and signaling. *J. Allergy Clin. Immunol.* 117: 979–987, 2006; quiz 988.
13. Beg, A. A. 2002. Endogenous ligands of Toll-like receptors: implications for regulating inflammatory and immune responses. *Trends Immunol.* 23: 509–512.
14. Ohashi, K., V. Burkart, S. Flohe, and H. Kolb. 2000. Cutting edge: heat shock protein 60 is a putative endogenous ligand of the toll-like receptor-4 complex. *J. Immunol.* 164: 558–561.
15. Martinon, F., V. Petrilli, A. Mayor, A. Tardivel, and J. Tschopp. 2006. Gout-associated uric acid crystals activate the NALP3 inflammasome. *Nature* 440: 237–241.
16. Liu, S., D. J. Gallo, A. M. Green, D. L. Williams, X. Gong, R. A. Shapiro, A. A. Gambotto, E. L. Humphris, Y. Vodovotz, and T. R. Billiar. 2002. Role of toll-like receptors in changes in gene expression and NF-κB activation in mouse hepatocytes stimulated with lipopolysaccharide. *Infect. Immun.* 70: 3433–3442.
17. Karin, M., and A. Lin. 2002. NF-κB at the crossroads of life and death. *Nat. Immunol.* 3: 221–227.
18. Witte, M. B., and A. Barbul. 2002. Role of nitric oxide in wound repair. *Am. J. Surg.* 183: 406–412.
19. Frank, S., M. Madlener, J. Pfeilschifter, and S. Werner. 1998. Induction of inducible nitric oxide synthase and its corresponding tetrahydrobiopterin-cofactor-synthesizing enzyme GTP-cyclohydrolase I during cutaneous wound repair. *J. Invest. Dermatol.* 111: 1058–1064.
20. Reichner, J. S., A. J. Meszaros, C. A. Louis, W. L. Henry, Jr., B. Mastrofrancesco, B. A. Martin, and J. E. Albina. 1999. Molecular and metabolic evidence for the restricted expression of inducible nitric oxide synthase in healing wounds. *Am. J. Pathol.* 154: 1097–1104.
21. Nussler, A., J. C. Drapier, L. Renia, S. Pied, F. Miltgen, M. Gentilini, and D. Mazier. 1991. L-arginine-dependent destruction of intrahepatic malaria parasites in response to tumor necrosis factor and/or interleukin 6 stimulation. *Eur. J. Immunol.* 21: 227–230.
22. Nussler, A. K., L. Renia, V. Pasquetto, F. Miltgen, H. Matile, and D. Mazier. 1993. In vivo induction of the nitric oxide pathway in hepatocytes after injection with irradiated malaria sporozoites, malaria blood parasites, or adjuvants. *Eur. J. Immunol.* 23: 882–887.
23. Saeftel, M., A. Krueger, S. Arriens, V. Heussler, P. Racz, B. Fleischer, F. Brombacher, and A. Hoerauf. 2004. Mice deficient in interleukin-4 (IL-4) or IL-4 receptor α have higher resistance to sporozoite infection with *Plasmodium berghei* (ANKA) than do naive wild-type mice. *Infect. Immun.* 72: 322–331.
24. Aktan, F. 2004. iNOS-mediated nitric oxide production and its regulation. *Life Sci.* 75: 639–653.
25. Seglen, P. O. 1976. Preparation of isolated rat liver cells. *Methods Cell Biol.* 13: 29–83.
26. Wang, H., X. Gao, S. Fukumoto, S. Tademoto, K. Sato, and K. Hirai. 1998. Post-isolation inducible nitric oxide synthase gene expression due to collagenase buffer perfusion and characterization of the gene regulation in primary cultured murine hepatocytes. *J. Biochem.* 124: 892–899.
27. De Vera, M. E., B. S. Taylor, Q. Wang, R. A. Shapiro, T. R. Billiar, and D. A. Geller. 1997. Dexamethasone suppresses iNOS gene expression by up-regulating I-κB α and inhibiting NF-κB. *Am. J. Physiol.* 273: G1290–G1296.
28. Kasibhatla, S., L. Genestier, and D. R. Green. 1999. Regulation of fas-ligand expression during activation-induced cell death in T lymphocytes via nuclear factor κB. *J. Biol. Chem.* 274: 987–992.
29. Burns, K., F. Martinon, C. Esslinger, H. Pahl, P. Schneider, J. L. Bodmer, F. Di Marco, L. French, and J. Tschopp. 1998. MyD88, an adapter protein involved in interleukin-1 signaling. *J. Biol. Chem.* 273: 12203–12209.
30. Tsuji, M., D. Mattei, R. S. Nussenzweig, D. Eichinger, and F. Zavala. 1994. Demonstration of heat-shock protein 70 in the sporozoite stage of malaria parasites. *Parasitol. Res.* 80: 16–21.
31. Hulier, E., P. Petour, G. Snounou, M. P. Nivez, F. Miltgen, D. Mazier, and L. Renia. 1996. A method for the quantitative assessment of malaria parasite development in organs of the mammalian host. *Mol. Biochem. Parasitol.* 77: 127–135.
32. Miyamoto, N., M. Mandai, I. Suzuma, K. Suzuma, K. Kobayashi, and Y. Honda. 1999. Estrogen protects against cellular infiltration by reducing the expressions of E-selectin and IL-6 in endotoxin-induced uveitis. *J. Immunol.* 163: 374–379.
33. Adachi, O., T. Kawai, K. Takeda, M. Matsumoto, H. Tsutsui, M. Sakagami, K. Nakanishi, and S. Akira. 1998. Targeted disruption of the MyD88 gene results in loss of IL-1- and IL-18-mediated function. *Immunity* 9: 143–150.
34. Pierce, J. W., R. Schoenleber, G. Jesmok, J. Best, S. A. Moore, T. Collins, and M. E. Gerritsen. 1997. Novel inhibitors of cytokine-induced IκBα phosphorylation and endothelial cell adhesion molecule expression show anti-inflammatory effects in vivo. *J. Biol. Chem.* 272: 21096–21103.
35. Mellouk, S., S. L. Hoffman, Z. Z. Liu, P. de la Vega, T. R. Billiar, and A. K. Nussler. 1994. Nitric oxide-mediated antiplasmodial activity in human and murine hepatocytes induced by γ interferon and the parasite itself: enhancement by exogenous tetrahydrobiopterin. *Infect. Immun.* 62: 4043–4046.
36. Frevert, U. 2004. Sneaking in through the back entrance: the biology of malaria liver stages. *Trends Parasitol.* 20: 417–424.
37. Singh, A. P., C. A. Buscaglia, Q. Wang, A. Levay, D. R. Nussenzweig, J. R. Walker, E. A. Winzeler, H. Fujii, B. M. Fontoura, and V. Nussenzweig. 2007. *Plasmodium* circumsporozoite protein promotes the development of the liver stages of the parasite. *Cell* 131: 492–504.
38. Iwami, K. I., T. Matsuguchi, A. Masuda, T. Kikuchi, T. Musikacharoen, and Y. Yoshikai. 2000. Cutting edge: naturally occurring soluble form of mouse Toll-like receptor 4 inhibits lipopolysaccharide signaling. *J. Immunol.* 165: 6682–6686.
39. LeBouder, E., J. E. Rey-Nores, N. K. Rushmere, M. Grigorov, S. D. Lawn, M. Affolter, G. E. Griffin, P. Ferrara, E. J. Schiffrin, B. P. Morgan, and M. O. Labeta. 2003. Soluble forms of Toll-like receptor (TLR)2 capable of modulating TLR2 signaling are present in human plasma and breast milk. *J. Immunol.* 171: 6680–6689.
40. Janssens, S., K. Burns, J. Tschopp, and R. Beyaert. 2002. Regulation of interleukin-1- and lipopolysaccharide-induced NF-κB activation by alternative splicing of MyD88. *Curr. Biol.* 12: 467–471.
41. Fukao, T., M. Tanabe, Y. Terauchi, T. Ota, S. Matsuda, T. Asano, T. Kadowaki, T. Takeuchi, and S. Koyasu. 2002. PI3K-mediated negative feedback regulation of IL-12 production in DCs. *Nat. Immunol.* 3: 875–881.
42. Liew, F. Y., D. Xu, E. K. Brint, and L. A. O'Neill. 2005. Negative regulation of toll-like receptor-mediated immune responses. *Nat. Rev. Immunol.* 5: 446–458.
43. Bongfen, S. E., R. Torgler, J. F. Romero, L. Renia, and G. Corradin. 2007. *Plasmodium berghei*-infected primary hepatocytes process and present the circumsporozoite protein to specific $CD8^+$ T cells in vitro. *J. Immunol.* 178: 7054–7063.